CORA

Cork Open Research Archive
Cartlann Taighde Oscailte Chorcaí

UCC

University College Cork, Ireland
Coláiste na hOllscoile Corcaigh

Accepted Manuscript

SYNTHESIS AND CHARACTERIZATION OF NANOCOMPOSITES BASED ON PANI AND CARBON NANOSTRUCTURES PREPARED BY ELECTROPOLYMERIZATION
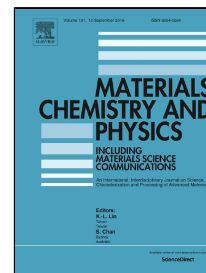
Aleksandar Petrovski, Perica Paunoviu0107, Roberto Avolio, Maria E. Errico, Mariacristina Cocca, Gennaro Gentile, Anita Grozdanov, Maurizio Avella, John Barton, Aleksandar Dimitrov

Highlights:

- Nanocomposites of PANI with carbon nanostructures were prepared for sensing application.

- By cyclic voltammetry, conductive form of PANI (green colored emeraldine phase) is obtained 0.75V

- Using 4 Probe method, nanocomposite PANI/CNS tablet was tested for sensing application

- Micro-structural properties of nanocomposites were studied by SEM, TGA and Raman analysis

SYNTHESIS AND CHARACTERIZATION OF NANOCOMPOSITES BASED ON PANI AND CARBON NANOSTRUCTURES PREPARED BY ELECTROPOLYMERIZATION

Aleksandar Petrovski[1], Perica Paunović[1], Roberto Avolio[2], Maria E. Errico[2],

Mariacristina Cocca[2], Gennaro Gentile[2], Anita Grozdanov*[1], Maurizio Avella[2],

John Barton[3], Aleksandar Dimitrov[1]

[1] - *Faculty of Technology and Metallurgy, SS Cyril and Methodius University,*

Rudjer Bošković, 16, 1000 Skopje, R. Macedonia

[2] - *Institute for Polymers, Composites and Biomaterials, National Research Council,*

Via Campi Flegrei 34, 80078 Pozzuoli, Napoli, Italy

[3] - *Tyndall national Institute, University College Cork, Dyke Parade, Cork, Ireland,*

T12 R5CP

*Corresponding author: Tel: +389 75 303 578 Fax:+389 2 3065 389

E-mail: anita.grozdanov@yahoo.com, anita@tmf.ukim.edu.mk

Abstract

Nanocomposites based on polyaniline (PANI) and carbon nanostructures (CNSs) (graphene (G) and multiwall carbon nanotubes (MWCNTs)) were prepared by *in situ* electrochemical polymerization. CNSs were inserted into the PANI matrix by dispersing them into the electrolyte before the electropolymerization. Electrochemical characterization by means of cyclic voltammetry and steady state polarization were performed in order to determine conditions for electro-polymerization. Electro-polymerization of the PANI based nanocomposites was carried out at 0.75 V vs. saturated calomel electrode (SCE) for 40 and 60 minutes. The morphology and structural characteristics of the obtained nanocomposites were studied by scanning electron microscopy (SEM) and Raman spectroscopy, while thermal stability was determined using thermal gravimetric analysis (TGA). According to the morphological and structural study, fibrous and porous structure of PANI based nanocomposites was detected well embedding both G and MWCNTs. Also, strong interaction between quinoidal structure of PANI with carbon nanostructures via $\pi-\pi$ stacking was detected by Raman spectroscopy. TGA showed the increased thermal stability of composites reinforced with CNSs, especially those reinforced with graphene.

Key words: Composite materials, Nanostructures, Raman spectroscopy, Thermogravimetry

1. Introduction

Among the various conductive polymers such as poly(p-phenylene), polythiophene, polypyrrole, poly-indole, polycarbazole, poly(p-phenylenevinylene), polyfluorene, polyaniline (PANI) has received great attention within the scientific community, due to its good environmental stability and unique properties such as electrical, electrochemical, electroluminescence, redox behavior, easy synthesis and low cost of its monomer precursor - aniline [1-5]. PANI can be found in several oxidation states such as completely reduced form − leucoemeraldine (Y = 1), completely oxidized form − pernigraniline (Y = 0), intermediate states − protoemeraldine (Y = 0.75), emeraldine base (Y = 0.5) and nigraniline (Y = 0,25) [5,6]. Emeraldine base is the most conductive form of polyaniline. Because of the unique fast redox and acid-base doping/dedoping properties, PANI has been considered as an appropriate electrode material for a variety of applications in electronic and optical devices, energy storage devices, supercapacitors, electrochromic devices, electron field emitters, sensors etc. [7-10]. However, its applications were restricted by its poor mechanical properties and low processability.

One of the most promising approaches to overcome the above limitations is using carbon nanostructures (CNS) as reinforcements in composites based on PANI matrix. CNSs (carbon nanotubes or graphene) are characterized by large surface area to volume ratio of the nanosized, sp^2 hybridized structure able to give of $\pi-\pi$ interactions with electron rich molecules of PANI matrix, improved electrical conductivity and high charge transfer. Thus, due to their unique mechanical, electronic and thermal

properties, CNSs have been used as appropriate building units for the development of PANI-nanocomposite materials with enhanced conductivity, thermal stability, and reinforcement properties [11-14].

CNS/PANI composites have been prepared using direct mixing methods, chemical and electrochemical polymerization [15]. In direct mixing methods, PANI and MWCNTs or graphene powders have been mixed by mechanical blending, mechanical stirring or sonication. In the chemical and electrochemical approaches, PANI nanocomposites have been produced by polymerization of aniline, mostly in acid solution. Chemical polymerization has been used when large quantity of polymer is requested, while electropolymerization is a proper way for the obtainment of polymer films [16]. In fact, electrochemical polymerization has been considered as an appropriate and flexible method for controlling the thickness and conductivity of the produced PANI or PANI nanocomposite film. To improve interfacial interactions between PANI and CNS, nanofillers should be previously functionalized in acid medium [17], in which carboxylic acid groups are produced at the defect sites of carbon nanostructures, thus improving the CNS dispersibility. However, a simple and quantitative method to prepare conducting CNS/PANI nanocomposites with controlled sizes is still lacking.

(Rev2: 1): Unlike other methods such as chemical polymerization where it is very difficult to obtain required pure form of PANI, electrochemical method offers opportunities to overcome this problem. In recent literature, scientist claim that obtained polyaniline by chemical polymerization always consists residues from other oxidized or reduced forms such as protoemeraldine or nigraniline. This is due to the difficulties to control the procedure conditions. In electrochemical method, quality of the product mostly depends from the applied potential.

4

Besides this, using electrochemical method it is possible to obtain nanocomposite directly on the screen printed electrode surface and avoiding the additional phase of dilution of the once obtained nanocomposite powder. Also, performing the electrochemical polymerization in H_2SO_4, PANI was doped during the chain forming and it was obtained in the conductive form.

Electrochemically prepared polymers or composites were considered good candidates as pH sensors due to the fact that they were strongly bonded to the electrode surfaces [18]. Due to the presence of amino groups in polymer chain, it was possible to chemically modify the electrodes to obtain potentiometric responses as a function of pH changes in aqueous solutions.

In this paper, CNSs/PANI nanocomposites were successfully produced by electrochemical polymerization in view of possible sensing applications (pH measurement and, indirectly, pCO_2 detection). Furthermore, the morphology, electrochemical and structural and thermal properties of the nanocomposites were investigated.

2. Experimental

2.1. Materials and processing

The CNSs/PANI nanocomposites were obtained *via* electrochemical polymerization of aniline in the presence of two different carbon nanostructures: graphene (G) or multi-walled carbon nanotubes (MWCNTs). The used graphene was produced in the labs of Faculty of Technology and Metallurgy by molten salt electrolysis using highly oriented graphite electrodes [19]. MWCNTs were used as received from JRC (No.231, ISPRA, d=10÷40 nm, purity ~ 94%). Before the electrolysis, graphene was

purified in 10 wt% solution of H_2O_2 for 2 h and further, in concentrated solution of HF (40 wt%) for 1 h.

(Rev.2, 5): Electrochemical polymerization of CNS/PANI was performed in standard electro-chemical cell of 250 cm^3 (ml), with a three electrode system. Platinum tiles with surface of 10 cm^2 were used as working and counter electrodes, while saturated calomel electrode (SCE) was used as reference electrode. The electrolyte contains 0.1 M aniline and 0.5 M H_2SO_4. Constant volume of aniline was used for all the experiments in order to avoid the differences. Carbon nanostructures, G or MWCNTs, were dispersed into the electrolyte by sonification (30 min) in an ultrasonic bath. The dispersion is stirred my magnetic stirrer (200 rpm) for the entire process of electrochemical polymerization. Before the electrochemical synthesis of PANI and PANI composites, cyclic voltammetry and steady-state polarization measurements were performed in order to optimize the experimental conditions. Further, electro-polymerization was carried out at constant potential of working electrode of +0.75 V vs. SCE until current reaches 110 mA. These data are determined from the electrochemical measurements (CV and SS). Within both the composite systems, G/PANI and MWCNTs/PANI, different samples were prepared varying the content of the CNS (1, 2 and 3 wt %) and the time of electro-polymerization (40 and 60 min). Nanocomposite powder for the tablet preparation was taken from Pt-electrode surface and additional doping in 0.1 M HCl was performed for 24 h in order to enrich maximum doping level. Further, the powder was filtered and washed out with distilled water several times. After drying at room temperature for 24 h, nanocomposites were pressed in the form of tablets and investigated with 4 probe method. Nanocomposite tablets for testing of sensing activity were prepared at the following conditions: (Rev2, 2)= 135 ℃, P=10 kN, t=10 min.

6

(Rev.3, 3): For the further testing of pH sensing, the CNS/PANI nanocomposites will be obtained directly on Screen Printed Electrode surface.

2.2. Characterization techniques

Structural characteristics of the obtained nanocomposite materials were studied by means of Raman spectroscopy. Non-polarized Raman spectra were recorded by a confocal Raman spectrometer (-Lab Ram ARAMIS, Horiba Jobin Yvon) operating with a laser excitation source emitting at 532 nm. Morphology of the nanocomposites was analyzed in high vacuum mode by means of a scanning electron microscope (SEM) FEI Quanta 200 using a secondary electron detector and acceleration voltage of 30 kV. Thermal stability of the materials was studied by means of thermogravimetric analysis (TGA) and differential thermal analysis (DTA). For TGA and DTA, a Perkin Elmer PYRIS Diamond Thermogravimetric/Differential Thermal Analyzer was used. In both cases, the samples were heated under nitrogen atmosphere, in the range 30-800 $^{\circ}$C with a heating rate of 20 $^{\circ}$C·min^{-1}. Electrical conductivity of the CNS/PANI tablets at different pH was followed using the 4 Probe Method (the 4 probes were fixed at 1mm apart).

3. Results and discussions

3.1 Electrodeposition of PANI and PANI composites

Cyclic voltammograms (CV) of the electropolymerization of aniline with and without CNSs in the electrolyte were recorded in the potential region from –0.2 to 1 V. The order of all steps of transformation from aniline to polyaniline was observed in the CV curves. CV spectra recorded for formation of pure PANI (electrolyte composition:

(Rev2, 3): 0.1 M aniline + 0.5 M H_2SO_4) and PANI composite with graphene G/PANI (electrolyte composition: 0.1 M aniline + 0.5 M H_2SO_4 + graphene, 2wt% related to the weight of aniline) are shown in Figure 1. Both spectra show almost the same shape, characteristic of PANI [20-23]. The spectrum of electro-polymerization of PANI in presence of graphene is more widespread than that without graphene due to higher currents registered. For this reason characteristic peaks in the spectra of pure PANI are not well pronounced as those for G/PANI. The same effect of several-fold higher currents was registered also in the CV spectra of MWCNT/PANI nanocomposites [15].

Fig. 1.

Table 1.

As result of considerably higher electroconductivity of graphene, growth of the composite on electrode is faster due to faster electrons exchange between ions and electrode. Position of the characteristic peaks in the voltammograms is shown in Table 1. Positions of the peaks of pure PANI show insignificant shift related to those of G/PANI composite. First oxidation peak denoted as P_1 corresponds to first step of oxidation of PANI, i.e. transformation of leucoemeraldine, base oxidation state of PANI (completely reduced, 0), to emeraldine, salt oxidation state of PANI (half reduced, +1) [22,23]. Corresponding redox peak P_1' is attributed to the reverse transformation. Redox pair denoted as P_2/P_2' can be attributed to formation of secondary products like benzoquinone/hydroquinone [22,23] or overoxidation or degradation of PANI [24]. The next redox pair P_3/P_3' corresponds to transformation of p-aminophenol/benzoquinonemine [24,25]. Redox pairs P_2/P_2' and P_3/P_3' appear when the cyclic voltammetry measurements are performed with higher anodic potentials than the next redox peaks P_4/P_4'. After P_4 peak degradation of PANI

8

occurs, thus, redox pairs P_2/P_2' and P_3/P_3' can be ascribed to oxidation and reduction of degradation products [20,26]. When voltammetry measurements are performed in lower potential region (before the appearance of anodic peak P_4), the redox pairs P_2/P_2' and P_3/P_3' can not be observed and the only redox pair which appears is P_1/P_1' [22]. Last oxidation peak P_4, corresponds to transformation of emeraldine salt oxidation state of PANI (half reduced, +1) to pernigranilline (completely oxidized state +2) [22, 23]. Formation of electroconductive PANI, i.e. G/PANI composite aimed for most of applications, occurs in the potential region from 0,64 to 0,8 V. Electropolimerization of PANI or G/PANI composite should be performed at potential on which partially oxidized emeraldine is produced, i.e. to avoid formation of fully oxidized PANI – pernigranilline. Namely, partially oxidized emeraldine with green color is a desired conductive form of PANI which has variety of application. Further oxidation of the green conductive emeraldine transforms it to fully oxidized dark blue perningraniline salt, with lower conductivity [16]. So, the working potential should be on the first half of the above mentioned potential region. In order to determine the working potential more exactly, the steady-state polarization measurement was performed. The obtained polarization curve is shown in Figure 2.

Fig. 2.

Fig. 3.

According to polarization curve, oxidation of emeraldine starts at 0.7 V, while complete oxidation to dark blue pernigraniline occurs at 0.9 V. At the half of the electrochemically region of emeraldine oxidation (0.8 V) dark blue film was obtained (Fig. 3a). So, the working potential must be lower. At 0.75 V green film was formed (Fig. 3b), which pointed out an electroconductive form of PANI. Thus, as a working

potential for electropolymerization of PANI and G/PANI composite 0.75 V vs. SCE was selected, which was in agreement with the results of other authors [27].

The current changes during the electro-polymerization of pure PANI, PANI based composites G/PANI and MWCNTs/PANI, are given in Figure 4. Obviously, during the electro-polymerization of CNSs/PANI systems, current density increased, which pointed out the autoaccelerating character of the process [28].

Fig. 4.

Increase of the current density was a result of continuous growth of polymer/composite film on the electrode with increased roughness of the surface [22]. At the beginning, the increase of the current density was not so pronounced because of the induction period of formation of PANI or PANI composite film. According to the literature [28-30], in this period several processes occurred, such as oxidation of aniline to radical cations, these radical cations are polymerized to oligomer of aniline and finally polyaniline was generated by autocatalytic reaction. After formation of initial PANI film, its growth was faster expressed with a pronounced increase of the current density. Formation of composites was more intensive than pure PANI. Incorporated carbon nanostructures within the polymer film, due to their higher electro-conductivity, promoted a faster exchange of electrons and consequently, higher current density. The composite with carbon nanotubes − MWCNT/PANI has shown the most intensive polymerization.

3.2 Morphological analysis

The morphology of the PANI composites was investigated by scanning electron microscopy and the obtained secondary electron images are shown in Figure 5. Generally, the SEM characterization of CNS/PANI nanocomposites has revealed a uniform wrapping of CNS by PANI [15,31]. For both types of composites, fibrous

and porous structure of PANI can be observed. In literature, it can be found that for deposition time of 20 minutes, fibrous structure of PANI was grown instead of granular one [31]. Deposition time of the presented composite samples was 40 min, thus, fibrous morphology was expected. In the PANI composite with graphene (G/PANI, Fig. 5a and b), the diameter of PANI fibers varied from 70 to 150 nm.

Fig. 5.

The morphology of MWCNT/PANI composite (Fig. 5 c and d) was similar to the previous one, but in this case, PANI fibers generally presented bigger diameter, from 200 to 450 nm. Moreover, in Fig. 5d, carbon nanotubes can be observed on the surface of PANI fibers and in some cases partially embedded in them, thus indicating good polymer/nanofiller interactions.

3.3 Raman spectroscopy

Raman analysis was performed to determine the structural characteristics of the carbon nanostructures and to confirm their interactions with the PANI polymer matrix.

Fig. 6.

In Fig. 6a, Raman spectra of neat graphene and MWCNTs are shown. D peaks characteristic for disordered carbon at 1329 cm^{-1} for graphene and 1348 cm^{-1} for MWCNTs were recorded. G peak characteristic for highly ordered carbon structure was registered at the same position for both materials at 1580 cm^{-1}. This is in accordance with the literature data [32-34]. For both carbon materials, D peak is considerably less intense than G peak. This means that both carbon nanostructures contain very low amount of defects and impurities. At 1622 cm^{-1} D' peak was detected, usually attributed to intercalated graphite compounds, increasing disorder by functionalization and strain in the C–C bond vibrations [34]. 2D peak at 2688 cm^{-1} is

11

the second order of the D band appearing as result of lattice vibrational process [35]. 2D was not attributed to the defects in the structure, but it was dependent on the number of graphene layers. The used graphene has shown very intense 2D peak, which suggested a few layered graphene (2–3 layers) [35].

In the Raman spectra of PANI composites (Fig. 6b), only two peaks were detected. The first peak was centered at 1293 cm^{-1} for both composites. It was derived from the convolution of the D band of the carbon nanostructures, originally centered at 1329 cm^{-1} for graphene and 1348 cm^{-1} for MWCNTs, with the PANI band characteristic for C–N bonding in semiquinoid and quinoid ring, usually centered at 1260 cm^{-1} [36]. The second peak, partially convoluted with the first one, was centered at 1521 cm^{-1} for MWCNT/PANI composite and 1514 cm^{-1} for G/PANI composite. These peaks correspond to the shift of G band of the carbon nanostructures, from 1580 cm^{-1} to 1521 cm^{-1} in case of MWCNTs/PANI and to 1514 in the case of G/PANI. The recorded shifts of the G peaks for carbon nanostructures has pointed out on strong interaction of graphene and MWCNT with the quinoidal structure of the polymer matrix via π–π stacking [37,39].

3.4 Thermal analysis

PANI composite should be applied on the electrode surface and baked at higher temperature, up to 500 $^\circ$C, to assemble the final sensor [15]. In order to determine high temperature stability, thermal analysis was performed using thermogravimetric analysis (TGA) coupled with differential thermal analysis (DTA).

Thermal stability of PANI and its nanocomposites affected by several important factors such as acid dopant, oxidation state of the polymer, monomer substitution, atmosphere of the heat treatment, exposure time and preparation conditions [40].

TGA curve of PANI is shown in the window of Fig. 7. TGA data obtained for PANI show three steps of degradation. The first one around 100 ^{o}C was obtained due to the moisture removal. The second one between 250 and 300 ^{o}C was attributed to the elimination of the low molecular weight oligomers and the dedoping process, while the third step of degradation was associated with the decomposition of PANI.

TGA curves of PANI composites with MWCNTs are shown in Fig. 7. The first inflection of the curves for all samples was around 100 ^{o}C which was related to moisture removal. Further, three characteristic temperatures were detected. The first one (T_{onset}) corresponds to the beginning of the thermal decomposition of the composites and was registered at the point of 2% weight loss of the sample (after complete water removal). The second one (T_{d1}) was related to the weight loss of the doped acid. The third temperature (T_{d2}) was attributed to the polymer backbone degradation of the composites and has indicated their thermal stability. The registered temperatures are summarized in the Table 2.

Fig. 7

Table 2.

In the MWCNT/PANI systems (Fig. 7a) it can be seen that the composite with 1 wt% MWCNTs has started to degrade at higher temperature (264°C), while the degradation of the other two composites with 2 and 3 wt% started at almost the same temperature. Variations in the T_{d1} could be attributed to the different dopant interactions with the material. Increasing the carbon nano content, T_{d1} decreased due to the smaller interactions among the dopant and the polymer matrix. According to the values of T_{d2} as an indicator of thermal stability, it can be concluded that the first composite with 1 wt% MWCNTs is the least stable (507.7 ^{o}C). The other composites with

increased amount of carbon nanostructure (2 and 3 wt%) expressed similar stability (528.1 °C and 527.3 respectively), higher than the first sample.

In the G/PANI systems (Fig. 7b), the temperatures of degradation are very close for all samples. The same trend for T_{d1} recorded for MWCNT/PANI was noticed for G/PANI nanocomposites. Also, it was noticed that the longer time of electro-polymerization resulted in decreasing effect of T_{d1} and smaller dopant/polymer matrix interactions. The thermal stability of the first sample (G/PANI 1, 2 wt% graphene) was found to be the lowest (529.2 °C), but slightly better than all composite containing MWCNT. As the amount of the graphene increases to 3 wt% (sample G/PANI 2), the thermal stability increases to 546.8 °C. The same effect of improvement of the thermal stability (546.5 °C) can be achieved by prolonging the duration of electropolymerization to 60 min (sample G/PANI 3, 2 wt% graphene). All samples exhibited sufficient thermal stability for the application of the sensor assembly, especially the last two samples (G/PANI 2 and G/PANI 3).

(Rev.3, 2) Comparing the both CNS/PANI systems (G/PANI and MWCNT/PANI nanocomposites), slightly better thermal stability and interfacial potential was obtained for the G/PANI nanocomposites. G/PANI nanocomposites exhibited slightly stronger electrical conductivity changes due to the pH variations, although the same tendency for resistivity behavior of pH variations was obtained for both CNS/PANI systems. Furthermore, pH sensing was study at various CNS concentration (2 and 3 %), and the slightly better sensitivity was obtained for the nanocomposites with 3% CNS.

Fig. 8.

The expected synergetic effect of CNS/PANI nanocomposites has been a motivating factor to perform research on sensors, based on the mechanical stability of carbon

nanostructures and the redox properties of PANI [15]. Sensing activity of the obtained CNS/PANI nanocomposites was tested on tablets (Fig. 8) prepared with 2% and 3% carbon nanostructure content. Electrical conductivity at different pH was followed using the 4 Probe Method (the 4 probes are fixed at 1mm apart). It was found that comparing to the pH neutral (pH=7) with R=5.8450 Ω.cm; - at lower pH (or acidic media) resistivity increased (pH=4, R=130.157 Ω.cm), while at higher pH (alkali media) resistivity decreased (pH=10, R=2.119 Ω.cm).

(Rev.3, 4) The changes of the electrical conductivity of CNS/PANI nanocomposites was followed with a cumulative modulation of pH which occurs as the H^+ increases to an equilibrium concentration (pH =-log $[H^+]$). When additionally, CO_2 is present in the water, than stronger changes of electrical conductivity are expected due to the fact that CO_2 (aq) reacts with water forming a carbonic acid ($H_2O + CO_2$ (aq) = H_2CO_3). When carbonic acid dissociates ($H_2CO_3 = H^+ + HCO_3^-$) there is increasing in the $[H^+]$ concentration. So, the effect of pH change in the electronic conductivity of PANI polymer was explained on the basis of different degree of protonation of the imine nitrogen atoms in the polymer chain. But, further analysis will be performed in this direction.

The obtained results were used for the further development of nanocomposite sensor based on electro-polymerization performed directly on screen printed electrode [41].

4. Conclusions

The research presented in this paper, was motivated by the idea to produce nano-structured sensor based on conductive polymers reinforced with carbon nanostructures for detection of pH and pCO2 variation. For this purpose preparation of PANI composites reinforced by graphene and MWCNTs and their characterization

was done According to the presented results, we could draw the following conclusions:

- According to the cyclic voltammetry and steady-state polarization measurements, it was found that potential at which green colored emeraldine base – the most conductive form of PANI, is obtained 0.75 V. The studied composites with G and MWCNTs were electrochemically deposited at the mentioned potential.

- During the electropolymerization current density increases which points out on autoaccelerating character of the process. Reinforcing CNS components within the polymer film, due to their higher electroconductivity, causes a faster exchange of electrons and consequently, higher current density. The composite with carbon nanotubes – MWCNTs/PANI shows the most intensive polymerization.

- SEM observation showed that carbon nanostructures (G and MWCNTs) sheets were uniformly dispersed within the network of PANI fibers which confirmed good wrapping of CNS by polymer matrix and consequently higher interaction between PANI and CNS. The diameter of PANI fibers varied from 70 to 150 nm in the composite with graphene and from 200 to 450 nm in the composite with MWCNTs.

- The high interaction between polymer matrix and carbon based reinforcing components was proved by Raman spectra. Characteristic bands for carbon nanostructures were considerably shifted to lower values, close to characteristic bands of PANI, indicated the strong interaction between quinoidal structure of the PANI polymer matrix with carbon nanostructures, – MWCNTs and graphene via π–π stacking.

- Thermal analysis showed high thermal stability of the PANI composites with respect to the neat PANI. Graphene based composites showed higher temperature of decomposition than those with MWCNTs. Thermal stability of all studied composites is appropriate for further preparation of sensor assemblies for detection of pH and temperature variation.

- Electrical conductivity at different pH was followed using the 4 Probe Method. It was found that comparing to the pH neutral (pH=7, with R=5,8450 Ω.cm); - at lower pH (or acidic media) resistivity increased (pH=4, R=130,157 Ω.cm), while at higher pH (alkali media) resistivity decreased (pH=10, R=2,119 Ω.cm).

Acknowledgments

References

[1] E. Hermelin, J.Petitjean, S. Aeiyach, J.C. Lacroix and P.C. Lacaze, (Rev.2; 4)
J. Appl. Electrochem., 31 (2001) 905-911.

[2] B.Wessling,J.Posdorfer, Electrochem Acta, 44 (1999) 2139-2147.

[3] C. H. Chen, J. Appl. Polym. Sci., 89 (2003) 2142-2148.

[4]   Handbook of Organic Conductive Molecules and Polymers, Volumes 1–4, Wiley, New York, 1997.

[5]   M. Angelopoulos, R. Dipietro, W. G. Zheng, A. G. MacDiarmid, A. J. Epstein, J. Synth. Met. , 84 (1997) 35-39.

[6]   R. Ansari, M. B. Keivani, Polyaniline Conducting Electroactive Polymers: Thermal and Environmental Stability Studies, E-Journal of Chemistry, 3(4) (2006) 202-217.

[7]   J. Huang, S. Virji, B. Weiller, R.B. Kaner, Chem-Eur. J., 10 (2004) 1314-1319.

[8]   B.J. Gallon, R.W. Kojima, R.B. Kaner, P.L. Diaconescu, Angew.Chem., Int. Ed., 46 (2007) 7251-7254.

[9]   V. Gupta, N. Miura, Mater. Lett., 60 (2006) 1466-1469.

[10] T. Kobayashi, H. Yoneyama, H. Tamura, J. Electroanal. Chem. 161 (1984) 419.

[11] S. B. Kondawar, M. D. Deshpande, S. P. Agrawal, Int. J. Compos. Mater., 2(3) (2012) 32-36.

[12] C. Oueiny, S. Berlioz, F. X. Perrin., Progress in Polymer Science, 39(4)(2014) 707-748.

[13] X.L. Xie, Y. W. Mai, X.P. Zhou, Mater. Sci. Eng., 49 (2005) 89-112.

[14] J. Sandler, M. S. P. Shaffer, T. Prasse, W. Bauhofer, K. Schulte, A. N. Windle, Polymer, 40 (1999) 5967-5971.

[15] P. Gajendran, R. Saraswathi, Pure Appl. Chem., 80 (2008) 2377-2395.

[16] M. M. Gvozdenović, B. Z. Jugović, J. S. Stevanović, T. Lj. Trišović, B. N. Grgur, INTECH, Chap. 4. (ISBN 978-953-307- 693-5), (2011) 77-96.

[17] T.-M. Wu, Y.-W. Lin, C.-S. Liao, Carbon, 43 (2005) 734-740.

[18] B. Lakard, G. Herlem, S. Lakard, R. Guyetant, B. Fahys, Polymer 46 (2005) 12233-12239.

18

[19] A. T. Dimitrov, A. Tomova, A. Grozdanov, O. Popovski, P. Paunovic, J Solid State Electrochem, 17 (2013) 399-407.

[20] Lj.D. Arsov, W. Plieth, G. Koûmehl, J Solid State Electrochem, 2 (1998) 355-361.

[21] S. Pruneanu, E, Veress, I. MArian, L. Oniciu, J. Mater. Sci., 34 (1999) 2733-2739.

[22] I. Mickova, A. Prusi, Toma Grčev, Ljubomir Arsov, Bull. Chem. Technol. Macedonia, 25 (2006) 45-50.

[23] B.O. Taranu, E. Fagadar-Cosma, I. Popa, N. Plesu, I. Taranu, Digest Journal of Nanomaterials and Biostructures, 9(2) (2014) 667-679.

[24] H. K. Hassan, N. F. Atta, A. Galal, Int. J. Electrochem. Sci., 7 (2012) 11161-11181.

[25] J. Gu, S. Kan, Q. Shen, J. Kan, Int. J. Electrochem. Sci., 9 (2014) 6858-6869.

[26] E. Genies, M. Lapkowski, J. Penneau, J. Electroanal. Chem. Interfac. Electrochem., 249 (1988) 97-107.

[27] P. Gajendran, R. Saraswathi, Pure Appl. Chem., 80 (2008) 2377-2395.

[28] A. Malinauskas, J. Malinauskienë, CHEMIJA, 16(1) (2005) 1-7.

[29] S. Mu, J. Kan, J. Lu, L. Zhuang, J. Electroanal. Chem., 446 (1998) 107-112.

[30] H. Yang, A. Bard, J. Electroanal. Chem., 339 (1992) 423-449.

[31] H-J. Wang, P. Zhang, W-G. Zhang, S-W. Yao, Electrodeposition and characterization of polyaniline film, Chem. Res. Chinese Universities, 28 (2012) 133-136.

[32] A. C. Ferrari, J. C. Meyer, V. Scardaci, C. Casiraghi, M. Lazzeri, F. Mauri, S. Piscanec, D. Jiang, K. S. Novoselov, S. Roth, A. K. Geim, Phys. Rev. Lett. 97 (2006) 187401-1 – 187401-4.

[33] G. M. Morales, P.o Schifani, G. Ellis, C. Ballesteros, G. Martínez, C. Barbero, H. J. Salavagione, Carbon, 49 (2011) 2808-2816.

[34] J. H. Lehman, M. Terrones, E. Mansfield, K. E. Hurst, V. Meunier, Carbon, 49 (2011) 25812602.

[35] A. Ferrari, Solid State Communications, 143 (2007) 47-57.

[36] G. Varsanyi, Vibrational Spectra of Benzene Derivatives, Academic Press, New York, 1969.

[37] H. Yu, T. Wang, B. Wen, M. Lu, Z. Xu, C. Zhu, Y. Chen, X. Xue, C. Sun, M. Cao, J. Mater. Chem., 22 (2012) 21679-21685.

[38] Z. Tong, Y. Yang, J. Wang, J. Zhao, B-L. Su, Y. Li, J. Mater. Chem. A, 2 (2014) 4642-4651.

[39] C. Harish, V. Sai SreeHarsha, C. Santhosh, R. Ramachandran, M. Saranya, T. Mudaliar Vanchinathan, K. Govardhan, A. Nirmala Grace, Adv. Sci. Eng. Med., 5 (2013) 140-148.

[40] R. Ansari, M. B. Keivani, Polyaniline conducting electroactive polymers: thermal and environmental stability studies, E-Journal of Chemistry, 3(4) (2006) 202-217.

[41] J.A.S. Zamora, J. Barton, C. N. Cheallachain, J. Salat, P. Magni, P. Fanjul, J. Cleary, A. Grozdanov, F. Confalonieri, J. V. Gamboa, Y. Lassoued, C. Pizarro, J. Piwowarczyk, S. Heckmann, M. Challiss, E. Moynihan, 8th International Conference on Sensing Technology, Sep.2-4, (2014), Liverpool, UK, pp.204-209.
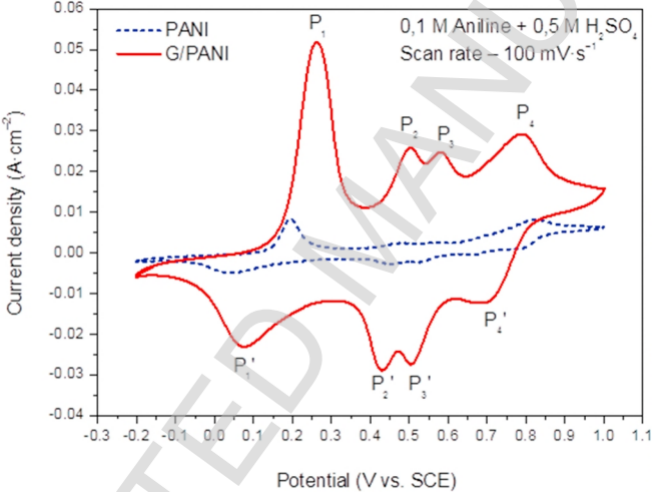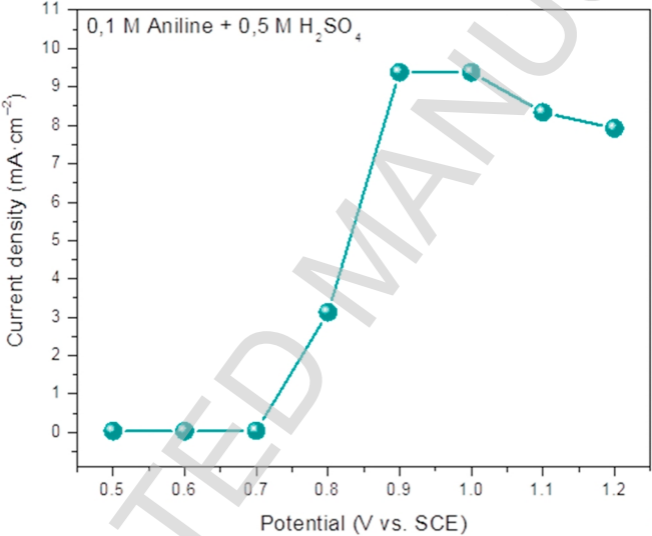
FIGURE CAPTION

Figure 1   Cyclic voltammograms of electrochemical formation of pure PANI (electrolyte composition: 0,1 M aniline + 0,5 M H_2SO_4) and PANI composite with graphene – G/PANI (electrolyte composition: 0,1 M aniline + 0,5 M H_2SO_4 + graphene, 2 wt%, related to the weight of aniline).

Figure 2   Steady-state polarization curve of electropolymerization of PANI (electrolyte composition: 0,1 M aniline + 0,5 M H_2SO_4).

Figure 3   a) Dark blue deposit of oxidized PANI b) green deposit of electroconductive PANI.

Figure 4   Change of current density during electropolymerization of pure PANI (electrolyte composition: 0,1 M aniline + 0,5 M H_2SO_4), G/PANI composite (electrolyte composition: 0,1 M aniline + 0,5 M H_2SO_4 + graphene, 2 wt%, related to the weight of aniline) and MWCNTs composite (electrolyte composition: 0,1 M aniline + 0,5 M H_2SO_4 + MWCNTs, 2 wt%, related to the weight of aniline).

Figure 5   SEM images of the studied PANI based composites a and b) G/PANI composite with 3 wt% graphene, c and d) MWCNTs/PANI composite with 3 wt% MWCNTs.

Figure 6   Raman spectra of a) used carbon nanostructures (graphene and MWCNTs) and PANI, and b) PANI based composites with 3 wt% carbon nanostructure.

Figure 7   TGA curves of a) MWCNTs/PANI and b) G/PANI composites. MWCNTs/PANI 1 – 1 wt% MWCNTs, MWCNTs/PANI 2 – 2wt% MWCNTs, MWCNTs/PANI 3 – 3 wt% MWCNTs, all deposited for 40 min. G/PANI 1 – 2 wt% graphene, G/PANI 2 – 3 wt% graphene, all deposited for 40 min and G/PANI 3 – 2 wt% graphene, deposited for 60 min.
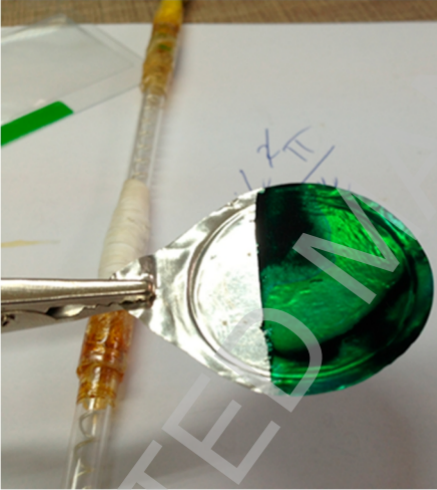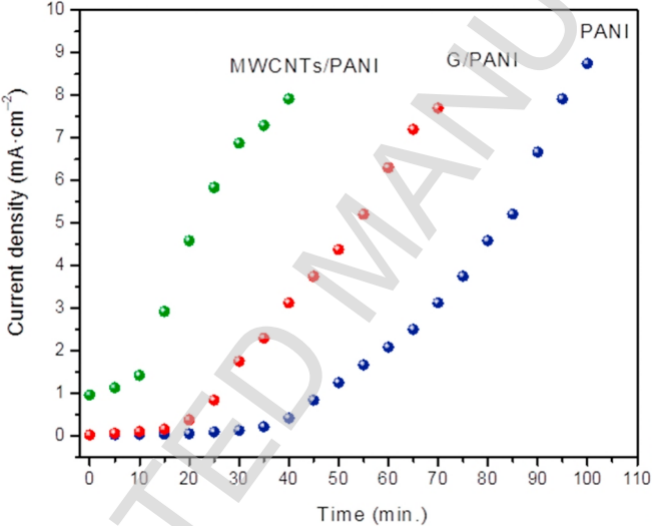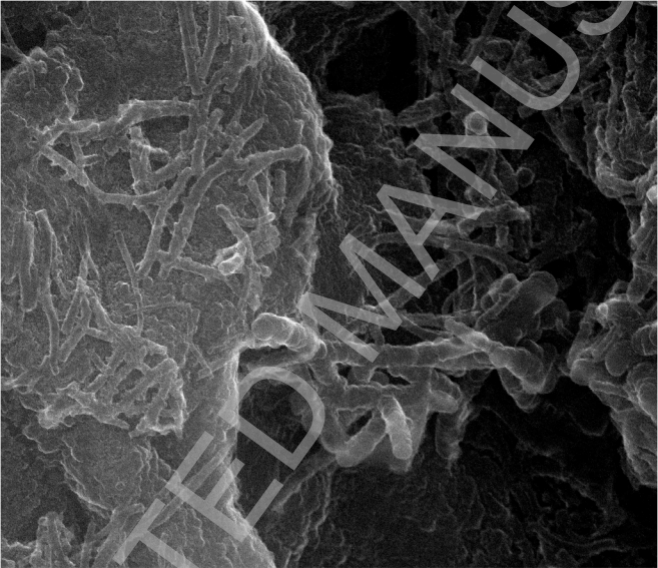
Figure 8   PANI/G nanocomposite tablet

Figure: Plot of Current density (mA·cm^{-2}) versus Potential (V vs. SCE) for 0,1 M Aniline + 0,5 M H$_2$SO$_4$.

HV	HFW	det	mag □	spot	WD		3 µm
30.00 kV	7.46 µm	ETD	40 000 x	1.5	10.4 mm		KG_5

HV	HFW	det	mag ☐	spot	WD	3 µm
30.00 kV	7.46 µm	ETD	40 000 x	1.5	10.4 mm	KG_5

HV	HFW	det	mag □	spot	WD	3 µm
30.00 kV	7.46 µm	ETD	40 000 x	1.5	10.7 mm	KC_5

HV	HFW	det	mag ⊡	spot	WD	1 µm
30.00 kV	3.73 µm	ETD	80 000 x	1.5	10.7 mm	KC_5

Y-axis: Mass, %
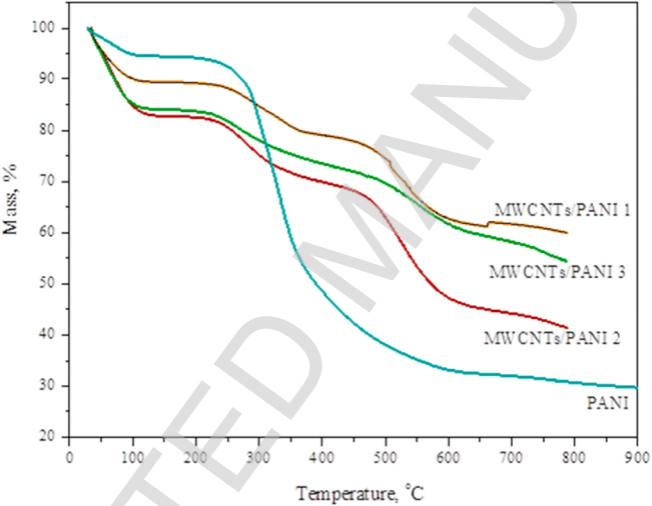
X-axis: Temperature, ℃

MWCNTs/PANI 1

MWCNTs/PANI 3

MWCNTs/PANI 2
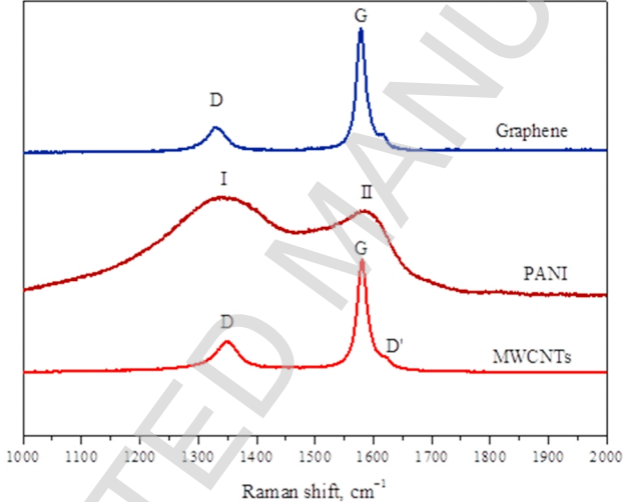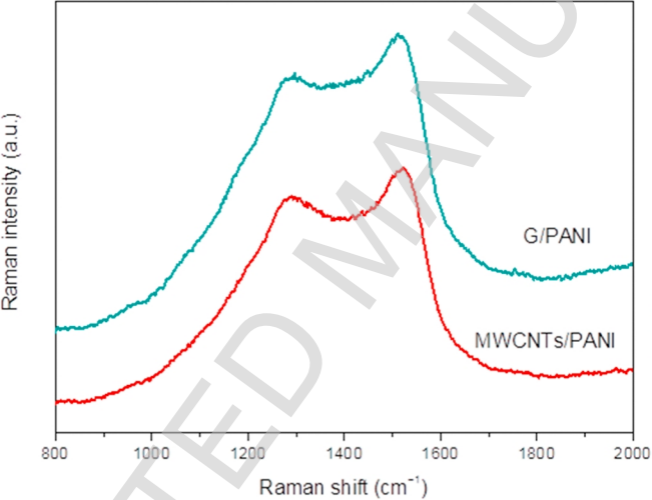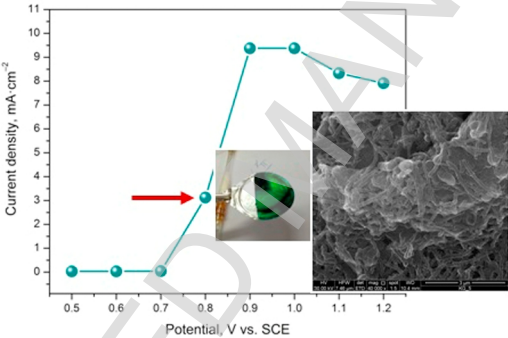
PANI
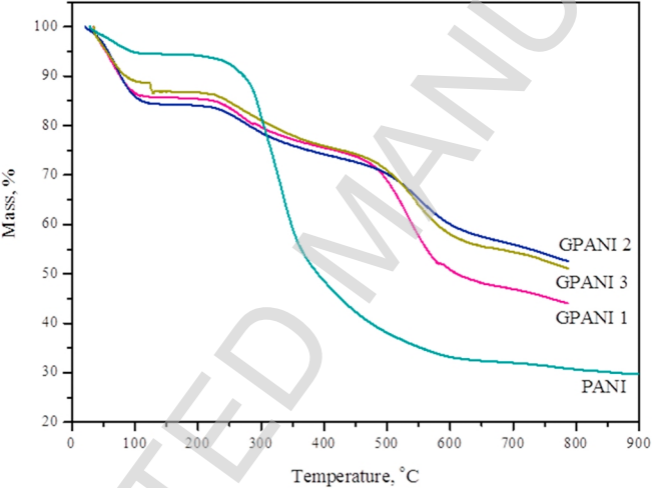
Table 1 Position of characteristic peaks (V) for PANI and G/PANI composite registered by cyclic voltammetry

	P_1	P_1'	P_2	P_2'	P_3	P_3'	P_4	P_4'
PANI	0.19	0.037	0.48	0.45	0.56	0.52	0.82	0.79
G/PANI	0.26	0.076	0.50	0.43	0.58	0.50	0.79	0.70

Table 2 Characteristic TG temperatures registered for different PANI composites

	$T_{onset.}$, ^{o}C	T_{d1}, ^{o}C	T_{d2}, ^{o}C
MWCNTs/PANI 1 (1 wt%, MWCNTs, 40 min)	264	332.9	507.7
MWCNTs/PANI 2 (2 wt%, MWCNTs, 40 min)	252	273.3	528.1
MWCNTs/PANI 3 (3 wt%, MWCNTs, 40 min)	251	278.5	527.3
G/PANI 1 (2 wt%, G, 40 min)	248.6	288.6	529.2
G/PANI 2 (3 wt%, G, 40 min)	249.5	271.3	546.8
G/PANI 3 (2 wt%., G, 60 min)	251.2	268.8	546.5